

Development of a Construction Material for Indoor and Outdoor, Metakaolinite-Based Geopolymer, with Environmental Properties

M. Mondragón-Figueroa¹, Héctor. R. Guzmán-Carrillo¹, Miguel Ángel Rico², José Luis. Reyez-Araiza³, Jorge. Pineda-Piñón⁴, Edgar J. López-Naranjo⁵, María C. Columba-Palomares⁶, José. M. López-Romero¹, José. Ramón Gasca-Tirado⁷ and Alejandro. Manzano-Ramírez¹

1. CINVESTAV-Querétaro, Libramiento Norponiente # 2000, Fraccionamiento Real de Juriquilla, Querétaro 76230, Qro., México

2. Facultad de Química, Universidad Autónoma de Querétaro centro de estudios Académicos sobre contaminación Ambiental, Querétaro 76010, Qro., México

3. DIPFI, Facultad de Ingeniería, Universidad Autónoma de Querétaro, C. U. Cerro de las Campanas, Centro, Querétaro 76010, Qro., México

4. Instituto Politécnico Nacional, Centro de Investigación en Ciencia Aplicada y Tecnología Avanzada, Unidad Querétaro, Cerro Blanco No. 141, Colinas del Cimatario, Querétaro 76090, Qro., México

5. DIP-CUCEI, Universidad de Guadalajara, José Guadalupe Zuno # 48, Los Belenes, Zapopan 45100, Jal., México

6. Facultad de Farmacia, Universidad Autónoma del Estado de Morelos, Av. Universidad # 1001, Cuernavaca 62209, Mor., México

7. Departamento de Ingeniería, Universidad de Guanajuato, Guanajuato 36000, México

Abstract: Environmental problems that came from the human activity have many facets, since pollution of the atmosphere arises from vehicles, industrial emissions while pollution of water could be from organic compounds, pesticides etc. These can cause serious health effects, such as respiratory diseases, including asthma and lung cancer. Hence, in the present work, a kinetic study on the effective adsorption and photo degradation of methylene blue (MB) dye, under ultraviolet A (UVA) irradiation of an alkali activated inorganic polymer (geopolymer) with homogeneously dispersed titanium dioxide (TiO₂) micro-particles is presented. In addition, antimicrobial testing of the alkali activated TiO₂ material was performed showing a bacteriostatic effect.

Key words: Heterogeneous photocatalysis, semiconductor, alkali activated, bacteriostatic effect.

1. Introduction

Photocatalysis and especially heterogeneous photocatalysis have been growing rapidly in the past three decades since in the degradation of organic compounds; semiconductor micro-particles may be involved as the incident light may initiate light-induced redox reactivity. On the other hand, alkali activated materials have gained, in the past fifteen years, a major interest so that the applications

of these materials comprise the development of new ceramics, cement and high-tech materials [1]. However, the versatility of this type of materials continues to give them new applications in different areas, for example in fire protection [2], immobilization of waste and toxic materials [3], radioactive waste encapsulation [4], building materials with antimicrobial activity [5], and biomedical materials [6], photoluminescent materials and for volatile organic degradation by photocatalysis [7] as well as on the study and development of photoactive composites along titanium dioxide (TiO₂). TiO₂ is an

Corresponding author: A. Manzano-Ramírez, Ph.D., professor, research fields: nanomaterials and ceramics.

excellent catalyst due to its strong oxidative potential, especially when exposed to ultraviolet (UV) light [8-13]. Thus, it has been used to remove organic dyes from water [14-19]. Finally, adsorption studies on geopolymer based materials have been carried out to evaluate their potential as photocatalyst for the removal of methylene blue (MB) from wastewater [20], for instance.

Hence, the main aim of the present work was to evaluate the photocatalysis capacity of a metakaolinite-based geopolymer composite with TiO_2 micro-particles by the adsorption and decomposition of MB in aqueous solution. The results showed a decay rate (k) with good pseudo-second order kinetics along the photocatalytic activity. In addition, bacteriostatic effect against commercially important bacteria was also observed.

2. Experimental Setup

2.1 Materials and Methods

Kaolin from Tizayuca, Hidalgo, Mexico was used. The chemical composition (weight percentage) of kaolin determined by X-ray fluorescence was: 73.19% SiO_2 , 24.80% Al_2O_3 , 1.26% SO_2 , and others. Commercial metakaolin was Metamax from BASF Corporation with the following chemical composition obtained from X-ray fluorescence 51.55% SiO_2 , 44.78% Al_2O_3 , 0.48% Fe_2O_3 , and others. Sodium hydroxide and sodium silicate were purchased from SIDESA-Corporation Mexico.

2.2 Geopolymer Preparation

DSC (differential scanning calorimetry) analysis was performed to determine the temperature at which complete dehydroxylation of kaolin and formation of metakaolinite take place. According to DSC results, it was detected that these processes occur at 548 °C, considering a heating time of 2 h. Thus, to ensure full kaolin dehydroxylation, the calcination of kaolin was

carried out at 700 °C for 2 h. The conversion of kaolinite to metakaolinite was confirmed by X-ray diffraction (XRD). Geopolymer samples were prepared by mechanically mixing stoichiometric amounts of metakaolin, sodium hydroxide, distilled water, sodium silicate ($\text{Na}_2\text{O}/\text{SiO}_2$ wt ratio: 0.18) and TiO_2 micro-particles with an average size of 358 nm, at three different weight percent concentrations: 0, 20 and 50 (samples: Geo cal, Geo 80-20 and Geo 50-50 respectively). Then, samples were subjected to 5 min of vibration, to produce homogenous slurry that was poured into cylindrical acrylic molds. The slurry was dried for 5 h at 70 °C and cured in a laboratory oven at 35 °C for 16 h. After cooling, geopolymers were obtained. The mixture constituents were formulated to follow the molar oxide ratios: $\text{SiO}_2/\text{Al}_2\text{O}_3 = 5.49$, $\text{Na}_2\text{O}/\text{SiO}_2 = 0.18$, $\text{Na}_2\text{O}/\text{Al}_2\text{O}_3 = 1.01$ and $\text{H}_2\text{O}/\text{Na}_2\text{O} = 18.39$.

When commercial metakaolin was used (Geo cMK), it was mixed directly with the same molar ratios indicated above, dried and cured at the same time and temperature.

The nomenclature and the weight percentages of TiO_2 used in this work for each set of samples are shown in Table 1.

2.3 Photocatalytic Degradation of MB

UV spectrometric techniques were used to study the adsorption and photochemical degradation of MB. A UV-Vis double beam spectrophotometer (Agilent 8453) at room temperature in the wavelength range 200-1,100 nm was used. The UV-Vis calibration curve for aqueous MB, was obtained using five different concentrations of MB, i.e., 0.45×10^{-5} , 0.85×10^{-5} , 1.0×10^{-5} , 1.4×10^{-5} and 1.8×10^{-5} M at the natural pH of the solution, relating the absorbance to the concentration as indicated in Table 2. The experiments were conducted under a UVA lamp ($\lambda_{\text{max}} = 340$ nm), 14 w.

Table 1 Weight percent of TiO₂ micro-particles in each set of samples.

Sample	Geo cal	Geo cMK	Geo 50-50	Geo 80-20
TiO ₂ micro-particles wt%	none	none	50	20

Table 2 MB-aqueous solutions used to obtain MB calibration curve and its corresponding absorbance values.

Concentration	Absorbance
0.45×10^{-5} M	0.29992
0.85×10^{-5} M	0.58384
1.0×10^{-5} M	0.66787
1.40×10^{-5} M	0.87075
1.80×10^{-5} M	1.13070

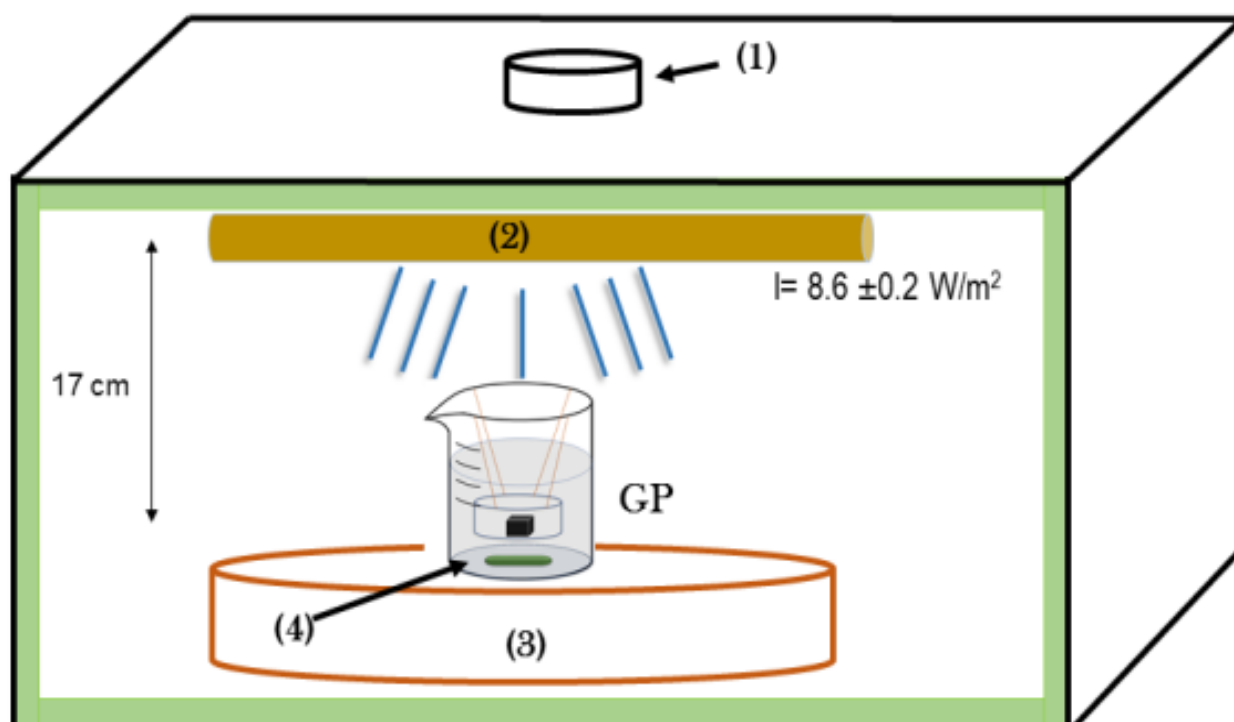


Fig. 1 Experimental set up for the adsorption and photodegradation of MB: (1) fan, (2) UVA lamp, (3) stirring plate, (4) stirrer.

A stock solution was prepared by weighing 0.01628 g of MB diluted in 500 mL of deionized water. Then the stock solution 8.36 mL was used to prepare 100 mL of a solution of MB at a concentration of 0.85×10^{-5} M which, then was poured into a 200 mL glass beaker (Pyrex) with circular geopolymer sample, 12.5 mm diameter, 2.6 mm thickness, and placed into the UV lamp system with a magnetic stirrer (Fig. 1). The distance between the liquid surface and the lamp was 17 cm.

For each measurement a 4 mL aliquot, deposited in

a 15 mL falcon tube was taken and placed in a premiere centrifuge, Model: XC-2009, operated at a speed of 3,500 rpm for a time of 5 min, and then a 3 mL sample was taken and placed into quartz cells of 3.5 mL volume and 1.0 cm trajectory length. Absorbance was measured at a wavelength of 664 nm that corresponds to the maximum absorption wavelength of MB, at times of 5 min during the first 20 min. After twenty minutes, measurements were taken every 10 min up to 100 min and its absorbance was measured.

To determine the adsorption equilibrium time, the experiment was conducted in dark conditions, thereafter the degradation was divided into two steps, adsorption in dark and photodegradation under UV illumination. Hence, each set of samples (i.e. Geo cal, Geo cMK, Geo 50-50, Geo 80-20) was subjected to these experimental conditions. All experiments were done in triplicate to ensure reproducibility of the methodology, and their average values were taken and plotted into graphs.

2.4 Textural Properties

The Brunauer-Emmett-Teller (BET) surface area, total pore volume and pore size distribution of the four samples were determined by nitrogen adsorption under $-190\text{ }^{\circ}\text{C}$ using a NOVAtouch LX gas sorption analyzer (Quantachrome Corp.). All samples were degassed at $200\text{ }^{\circ}\text{C}$ for 3 h, prior to the adsorption experiments. The BET surface area was obtained by applying the BET equation to the adsorption data. The pore size distribution was obtained using BJH (Barrett, Joyner, and Halenda) method.

2.5 Antimicrobial Activity of Geopolymers

To evaluate the antimicrobial activity, standard strains of *Staphylococcus aureus* (ATCC 6538), *Staphylococcus aureus* (MRSA, ATCC 43300), *Salmonella typhimurium* (ATCC 14028), *Escherichia coli* (ATCC 8739), and *Streptococcus pyogenes* (ATCC 19615) were used. The bacterial strains were grown and maintained in nutrient agar for 24 h in the dark at $37\text{ }^{\circ}\text{C}$. The tubes were filled with 1 mL of a bacterial culture, grown overnight in 1 mL adjusted at

5×10^5 CFU/mL [21]. The test was conducted with 25 mg of the different geopolymer samples (sterilization by autoclaving). Gentamicin was used as positive control ($20\text{ }\mu\text{g/mL}$) (Pisa®); all the test tubes were incubated overnight at $37\text{ }^{\circ}\text{C}$ [22]. Following incubation, absorbance of the samples was checked at 600 nm using a microplate reader (GloMax®-Promega). Clear broth was used as blank. Bactericidal or bacteriostatic effect was determined by seeding a sample in Petri dishes (agar Mueller-Hinton).

Since the geopolymer samples with the semiconductor TiO_2 micro-particles were prepared with the calcined kaolin, for the antimicrobial tests, it was decided to compare the activity between the Geo cal, Geo 80-20, Geo 50-50 just.

3. Experimental Results

3.1 Adsorption and Photo-Degradation of MB by Metakaoline Based Geopolymer

It may be observed how the UV-Vis absorption spectrum obtained at 664 nm shows a linear dependence with MB concentration (Fig. 2).

To determine the adsorption equilibrium time, experiments were conducted in dark and under UVA irradiation.

The MB absorption spectra under UVA irradiation for 100 min at a MB concentration of 0.85×10^{-5} M for all the geopolymer samples are shown in Fig. 4.

Figs. 5 and 6 show the linear fit of the experimental data of the different geopolymers for the degradation of MB and the values of R^2 for each geopolymer while the kinetic parameters are shown in Table 3.

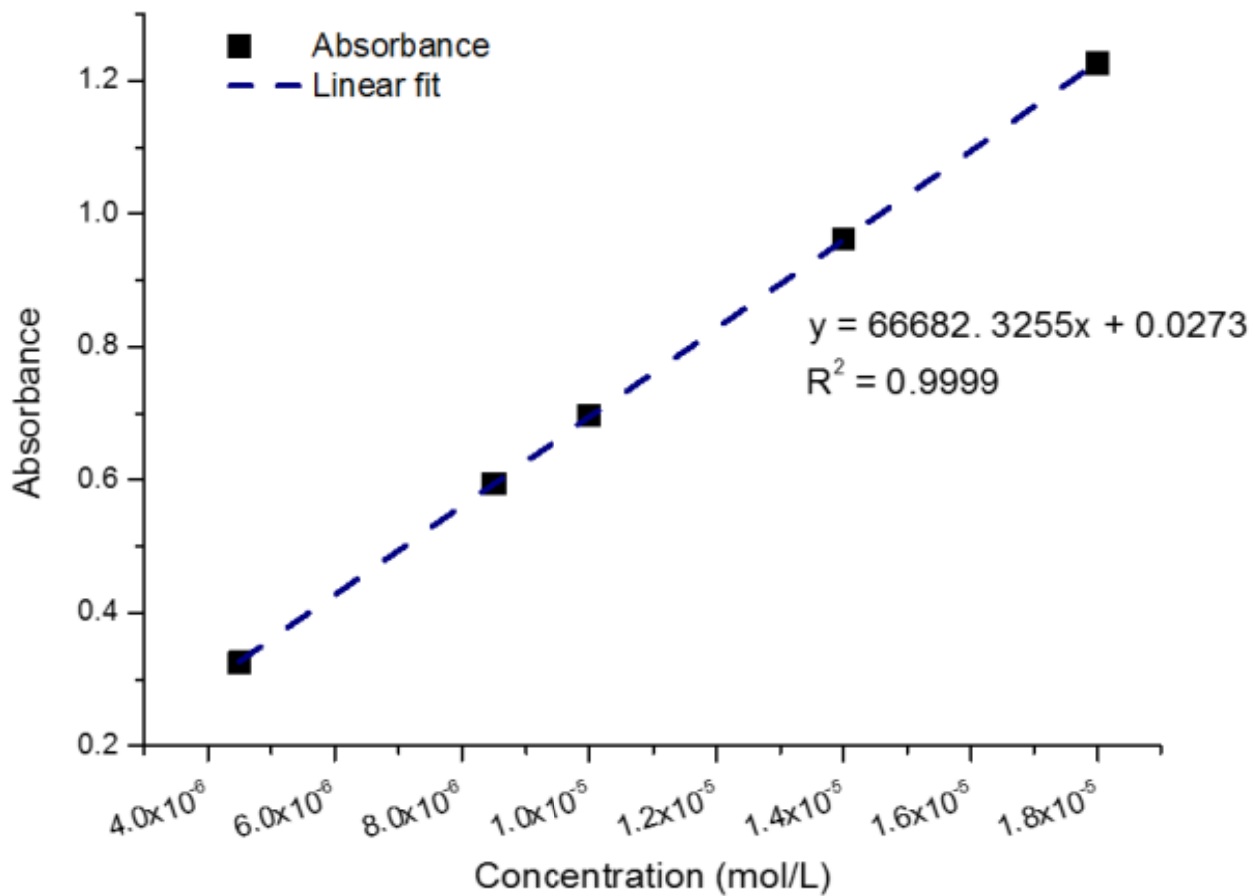


Fig. 2 UV-Vis calibration curve obtained from 664 nm intensity values.

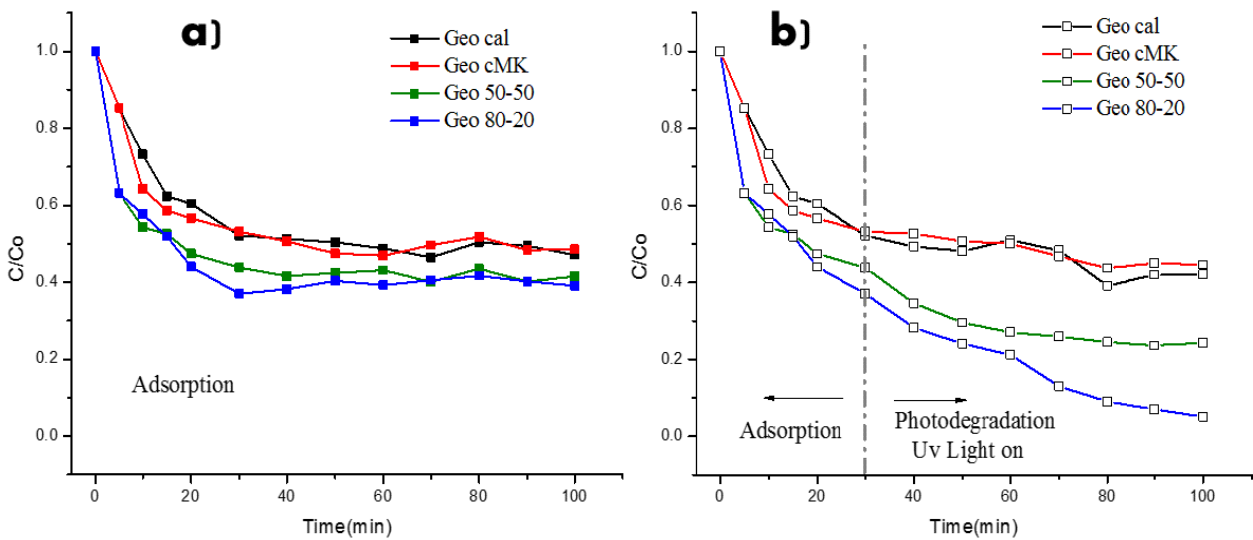


Fig. 3 Residual MB dye concentration vs. time of all geopolymers in (a) dark and (b) under UVA irradiation.

Development of a Construction Material for Indoor and Outdoor, Metakaolinite-Based Geopolymer, with Environmental Properties

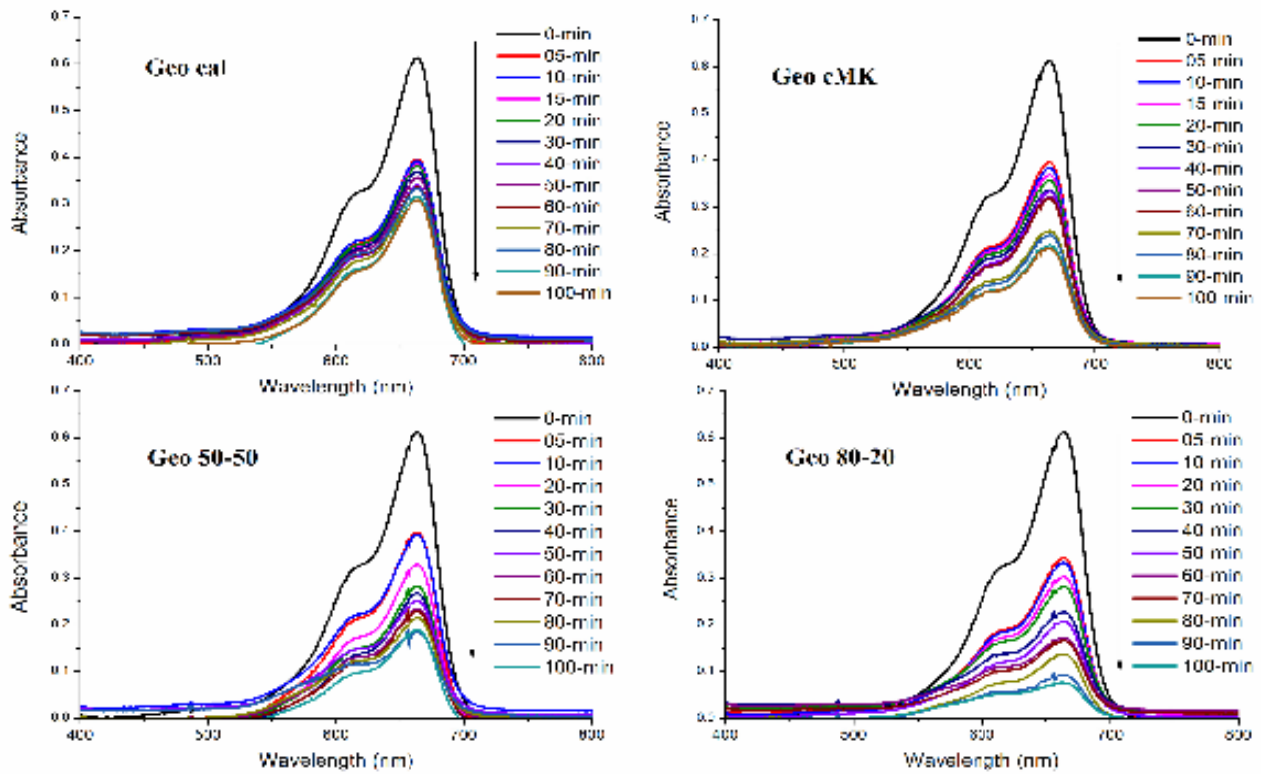


Fig. 4 UV-Vis absorption spectral changes of MB of geopolymer samples, after different reaction time under UVA irradiation.

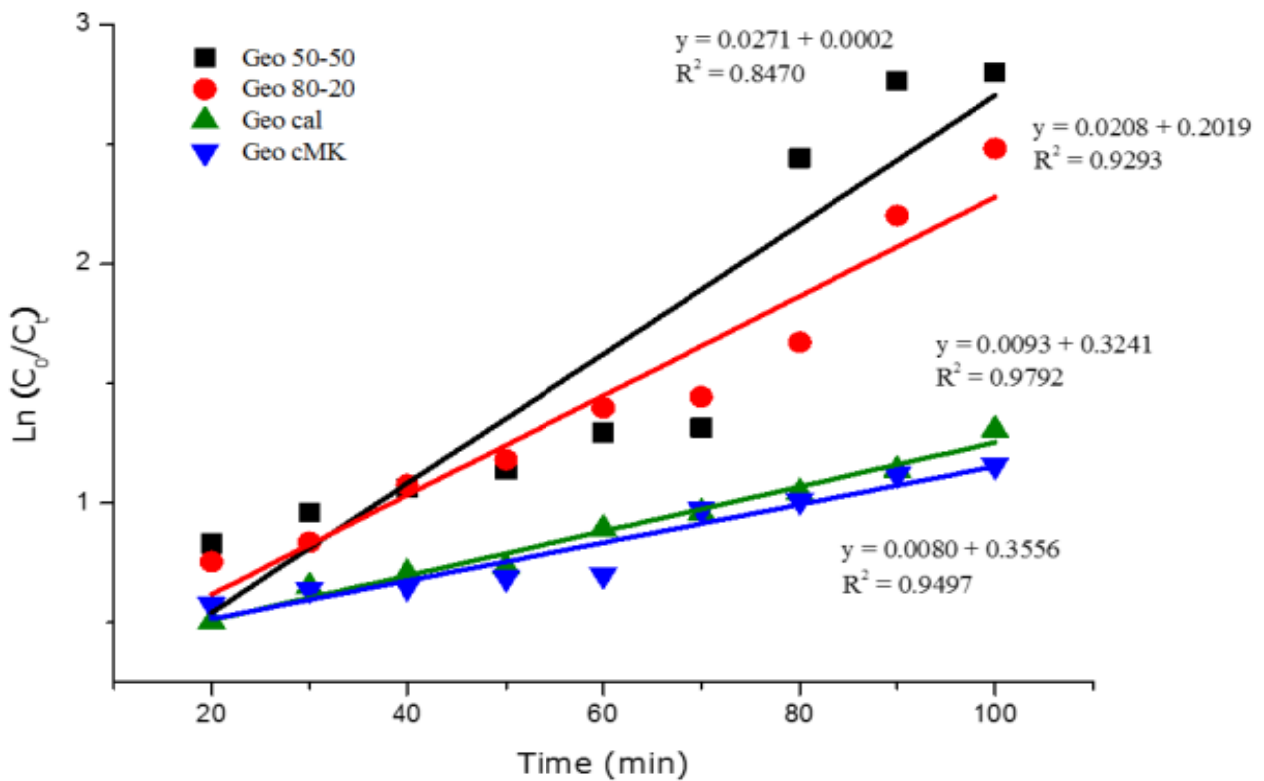


Fig. 5 Graphs of the pseudo-first order kinetics of MB adsorption on the different geopolymer composites with UVA irradiation.

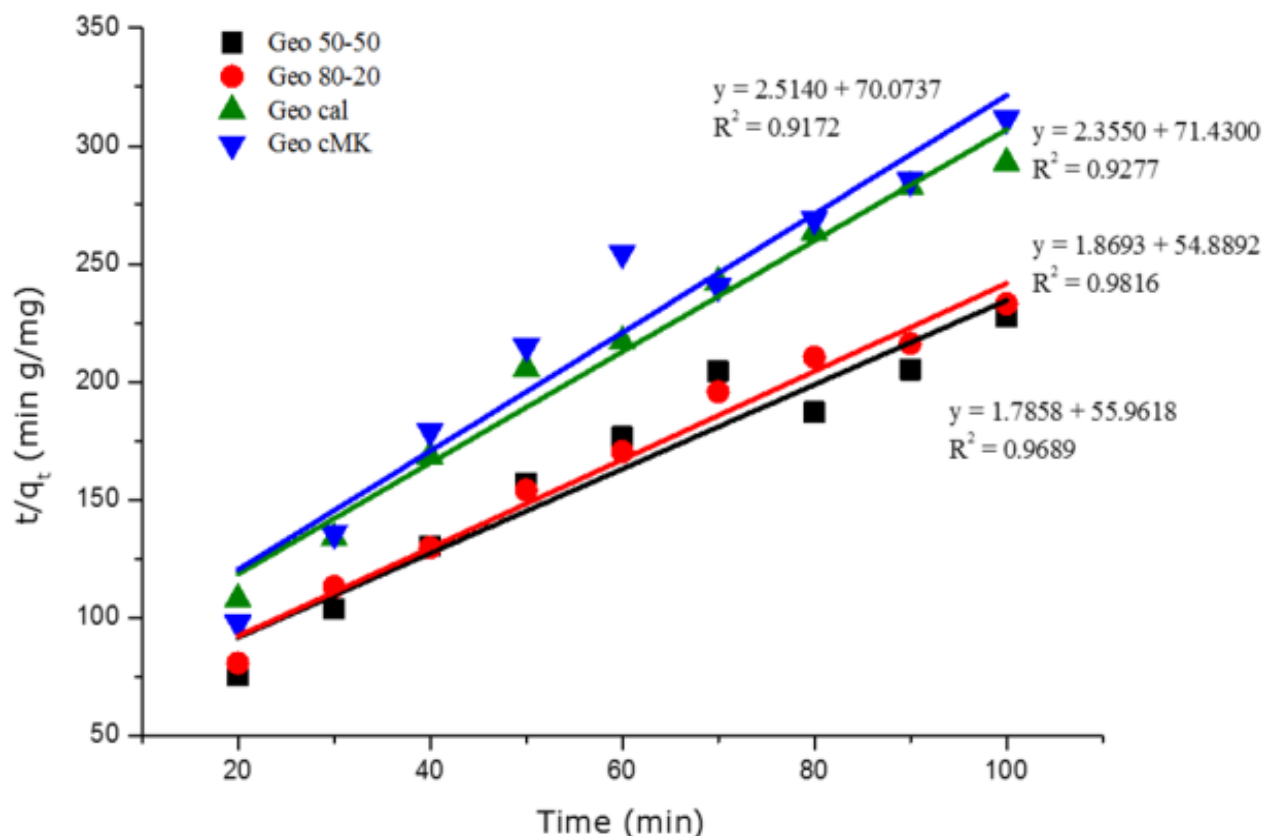


Fig. 6 Graphs of the pseudo-second order kinetics of MB adsorption on the different geopolymer composites with UVA irradiation.

Table 3 Parameters of the pseudo-first order and pseudo-second order kinetics models for the adsorption of MB on geopolymers.

Condition	Pseudo-first order kinetics parameters			Pseudo-second order kinetics parameters		
	k_1 (min^{-1})	q_e (mg/g)	R^2	k_2 (g/(mg min))	q_e (mg/g)	R^2
With additions						
Geo 50-50	0.0271	0.0070	0.8470	0.0570	0.5600	0.9689
Geo 80-20	0.0208	9.7120	0.9293	0.0637	0.5350	0.9816
Without additions						
Geo cal	0.0093	34.8600	0.9792	0.0776	0.4250	0.9277
Geo cMK	0.0080	44.4500	0.9497	0.0902	0.3980	0.9172

Table 4 Antimicrobial activity results of tested geopolymers.

Sample	% Inhibition				
	<i>Staphylococcus aureus</i> ATCC6538	<i>Staphylococcus aureus</i> ATCC 43300	<i>Salmonella typhimurium</i> ATCC 14028	<i>Escherichia coli</i> ATCC 8739	<i>Streptococcus pyogenes</i> ATCC 19615
Geo 50-50	13.06	34.75	NA	NA	NA
Geo 80-20	28.4	37.37	NA	24.44	NA
Geo cal	11.93	27.75	NA	8.66	8.62
Gentamicin	74.2	55	78.31	81.77	82.75

NA: non-active under testing conditions; ATCC: American type culture collection.

3.2 Antimicrobial Activity of Geopolymers

Table 4 shows the antimicrobial results of tested samples.

4. Discussions

It has been previously pointed out [14, 23] that the geopolymer efficiency as an absorber of organic dyes may be ascribed to the fact that hydroxyl groups present on the surface of the geopolymer may attract and hold cationic organic species [24]. Beaudon et al. [23] suggest that the cationic monomer and dimer species are initially adsorbed via cation exchange with Ca^{2+} onto anionic sites (in the present work the adsorption is suggested to occur mainly at the mesopores on the surface of the geopolymer) via an electrostatic attraction mechanism.

Fig. 4 shows visible spectra of MB dye after treatment with TiO_2 micro-particles under irradiation UVA at different reaction time for the geopolymer samples studied in the present work. There is no a clear hypsochromic effect as a result of N-demethylation in the spectra at low concentrations of MB [8]. To determine the adsorption equilibrium time, experiment was conducted in dark conditions and the results are shown in Fig. 3a. According to the results, it is possible to observe an equilibrium sorption-desorption after only 30 minutes, and this fast adsorption on the Geo cMK indicates that its use as an adsorbent is economically feasible since an adsorption process is preferred as an environmentally friendly and cost effective technique [25]. Generally, it is believed the higher surface area will result in

higher adsorption capacity because the adsorption capacity depends on the porous size and the surface properties. An increase in adsorption capacity of the materials without TiO_2 shows the following order for surface area values: Geo cMK > Geo cal (Table 5). On the contrary, the geopolymers with the addition of TiO_2 microparticles have a higher sorption capacity (q_e), even when the surface areas are minor than that of the geopolymers with no additions. This behavior is explained by the fact that the surface hydroxyl groups enhance interactions of the TiO_2 micro-particles with H_2O , which in turn presents a significant attraction effect of cationic dyes [23]. Fig. 3b shows the combined mechanism for the elimination of the cationic dye i.e., adsorption and photodestruction, these mechanisms occur in the geopolymers with TiO_2 micro-particles, however these two mechanisms are difficult to be distinguished.

For the geopolymers without TiO_2 , the concentration of MB follows a behavior similar to those in dark conditions. The small decrease in the values is ascribed to photolysis. It is essential to notice that when the lamp is on, the residual MB concentration reduces significantly because of photoactivation of the semiconductor micro-particles on and inside the geopolymermatrix, similar results are reported by trapping and holding dye molecules in the proximity to the oxides [16]. The rapid interaction between the MB solution and the geopolymer may be clearly illustrated by the absorption spectra of geopolymers in MB solution (with a 0.85×10^{-5} M concentration) (Fig. 4). In all the cases, very broad bands are observed as well as a light shift to the left in

Table 5 Textural properties of geopolymers.

Sample	S_{BET} (m^2/g)	V (cm^3/g)	D (nm)
Geo 50-50	1.473	0.020	4.684
Geo 80-20	1.649	0.022	3.416
Geo cal	2.374	0.048	3.022
Geo cMK	2.694	0.059	3.060

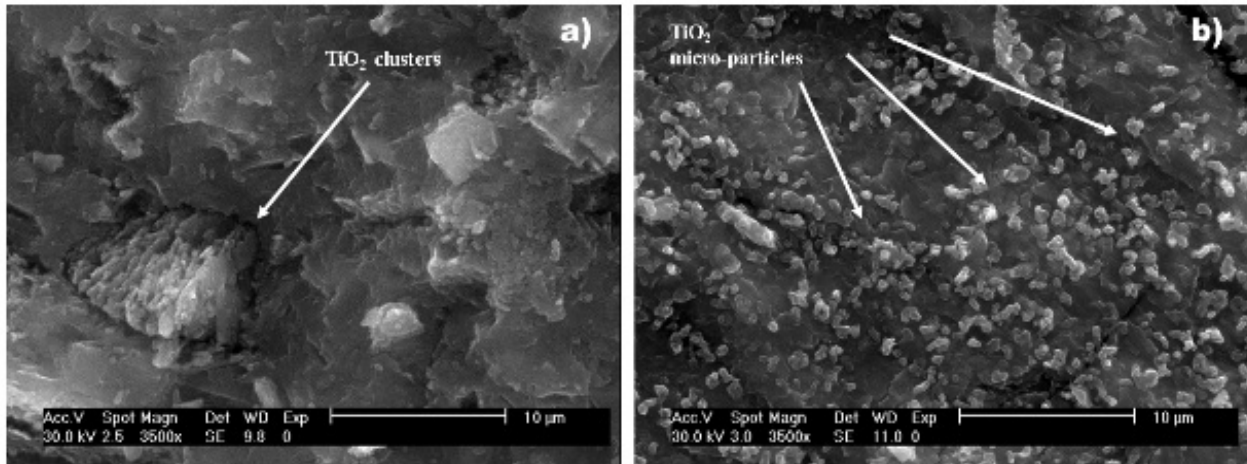


Fig. 7 SEM micrographics of the (a) Geo 50-50 with clusters of TiO₂ micro-particles and (b) well distributed TiO₂ micro-particles in the Geo 80-20.

the UV-Vis absorption band, phenomenon ascribed to the dye molecules interaction or adsorption with materials such as polyelectrolytes, anionic polymers or clay minerals [26-28]. In addition, the shoulder at approximately 610 nm can be related to the existence, in the MB solution, of free monomers (MB⁺) and dimers (MB⁺)₂ [23]. The rapid change in color from dark blue to light blue along a fast decrease of the absorption peak after 5 min reflects the high adsorption capacity of the geopolymers, being for the Geo 80-20 the highest (Fig. 3b).

To observe the impact of UV light on the degradation and the kinetics of the photocatalytic process by the different metakaolinite-based geopolymers, the experimental data were collected during 70 min after the first 30 min, the results were evaluated according to the pseudo-first equation law in the modeling of adsorption kinetics [29], Eq. (1) (Fig. 5), and pseudo-second order equations [19], Eq. (2) (Fig. 6).

$$\ln \frac{(q_e - q_t)}{q_e} = -k_1 t \quad (1)$$

$$\frac{t}{q_t} = \frac{1}{k_2 q_e^2} + \frac{1}{q_e} t \quad (2)$$

where q_e (mg/g) is the sorption capacity of MB at equilibrium and q_t (mg/g) is the sorption capacity at a time t , k_1 (min⁻¹) and k_2 (g/mg min⁻¹) are the rate constants for pseudo-first rate and pseudo-second

order respectively. By plotting $\ln(C_0/C_t)$ versus t , the pseudo-first rate constant k_1 and the equilibrium capacity (q_e) can be obtained from the slope and the intercept, respectively. Using the pseudo-second order equation, by plotting t/q_t versus t , the second-order rate constant (k_2) and the equilibrium capacity (q_e) are obtained from intercept and slop, respectively.

From Table 3, it may be observed that the correlation coefficients of MB absorbed for the Geo cal and Geo cMK which present the higher values of surface area (Table 5), fit well the pseudo-first order model suggesting that the main mechanism for the methylene blue discoloration is the physical adsorption [30] assuming the geopolymer solid remains constant while MB concentration decreases. In contrast, the correlation coefficients for the pseudo-second order model show much greater values for the samples with TiO₂ addition. In this model it is assumed the concentration of TiO₂ microparticles and geopolymer is constant, on the other hand, concentration of MB decreases over time. In the case of the Geo 80-20, the results evidence a true heterogeneous catalytic regime through photooxidation on the photocatalyst (TiO₂ micro-particles) which appears since the photonic excitation of the catalyst is the initial step. As the highest value is shown by the pseudo-second order rate equation ($R^2 = 0.9816$) with UV irradiation, it

may be inferred that the kinetics of the sorption rate does not depend on the concentrations of the demethylated intermediates formed (azure B and A) from MB degradation under UVA irradiation [10], but depends on the concentration of TiO₂ microparticles interacting with MB molecules. This means that the main mechanism for the discoloration of MB is by chemisorption [30] and photodegradation.

On the other hand, an excess of micro-particles of TiO₂ into the geopolymer results in a decrease in the kinetic rate value; this behavior could be related to a blocking of the active sorption sides [16] and agglomerations of the micro-particles (Fig. 7a) for Geo 50-50, which shows a non-homogeneous distribution of the micro-particles inside the matrix. In contrast, in Fig. 7b it is possible to observe TiO₂ micro-particles well distributed in the geopolymer Geo 80-20, which means a higher *k* value than Geo 50-50, hence, they reach equilibrium faster because the dye ions are adsorbed on the outer layers of the material while in the Geo 50-50 sample the dye ions will require long time and the equilibrium is slowly reached.

Finally, according to Table 4, samples showed a bacteriostatic effect to a different extent depending on the tested strain and TiO₂ content. Although TiO₂ has previously attracted a lot of attention due to its antibacterial properties in different applications, to the best of our knowledge, no antimicrobial tests had been carried out until now when used within a geopolymer matrix [31, 32]. According to the results, samples containing a higher weight percent concentration of TiO₂ showed a higher bacteriostatic effect. Furthermore, in accordance with previous works, TiO₂ seems to be particularly effective against *Staphylococcus aureus* [31].

5. Conclusions

The photocatalyst efficiency of a heterogeneous photocatalyst of different metakaolin-based geopolymers was studied by the removal of a model

cationic dye, methylene blue dye. In the case of the highest photocatalytic degradation of MB, geopolymer with the addition of 20 percent of TiO₂, is related to a combined mechanism: adsorption and semiconductor photodegradation effect. The removal efficiency of the MB on the surface of metakaolin based-geopolymers follows the pseudo-second order kinetics. The results indicate that because of its adsorbent behavior these materials are viable and environmentally friendly absorbent composites. Additionally, antimicrobial experiments showed how the tested samples present a bacteriostatic effect against commercially important bacteria.

References

- [1] Cioffi, R., and Maffucci, L. 2003. "Optimization of Geopolymer Synthesis by Calcinations and Polycondensation of a Kaolinitic Residue." *Resources, Conservation and Recycling* 40: 27-38. [https://doi.org/10.1016/S0921-3449\(03\)00023-5](https://doi.org/10.1016/S0921-3449(03)00023-5).
- [2] Giancaspro, J., Balaguru, P., and Lyon, R. 2004. "Fire Protection of Flammable Materials Utilizing Geopolymers." *Sample Journal* 40: 42-9.
- [3] Zhang, J. G., Provis, J. L., Feng, D. W., and Van Deventer, J. S. J. 2008. "Geopolymers for Immobilization of Cr⁶⁺, Cd²⁺, and Pb²⁺." *Journal of Hazardous Materials* 157: 587-98. <https://doi.org/10.1016/j.jhazmat.2008.01.053>.
- [4] Fernández-Pereira, C., Luna, Y., Querol, X., Antenucci, D., and Vale, J. 2009. "Waste Stabilization/Solidification of an Electric Arc Furnace Dust Using Fly Ash-Based Geopolymers." *Fuel* 88: 1185-93. <https://doi.org/10.1016/j.fuel.2008.01.021>.
- [5] Hashimoto, S., Machino, T., Takeda, H., Daiko, Y., Honda, S., and Iwamoto, Y. 2015. "Antimicrobial Activity Geopolymers Ion-Exchanged with Copper Ions." *Ceramics International* 41: 13788-92. <https://doi.org/10.1016/j.ceramint.2015.08.061>.
- [6] Wu, Y., Lu, B., Bai, T., Wang, H., Du, F., Zhang, Y., Cai, L., Jiang, C., and Wang, W. 2019. "Geopolymer, Green Alkali Activated Cementitious Material: Synthesis, Applications and Challenges." *Construction and Building Materials* 224: 930-49. <https://doi.org/10.1016/j.conbuildmat.2019.07.112>.
- [7] Mackenzie, K. J. D., and O'leary, B. 2009. "Inorganic Polymers (Geopolymers) Containing Acid-Base Indicators as Possible Colour-Change Humidity Indicators." *Materials Letters* 63: 230-2.

- <https://doi.org/10.1016/j.matlet.2008.09.053>.
- [8] Zhang, T., Oyama, T., Aoshima, A., Hidaka, H., Zhao, J., and Serpone, N. 2001. "Photooxidative N-Demethylation of Methylene Blue in Aqueous TiO₂ Dispersions under UV Irradiation." *Journal of Photochemistry and Photobiology A: Chemistry* 140: 163-72. [https://doi.org/10.1016/S1010-6030\(01\)00398-7](https://doi.org/10.1016/S1010-6030(01)00398-7).
- [9] Jafari, S., Zhao, F., Zhao, D., Lahtinen, M., Bhatnagar, A., and Sillanpää, M. 2015. "A Comparative Study for the Removal of Methylene Blue Dye by N and S Modified TiO₂ Adsorbents." *Journal of Molecular Liquids* 207: 90-8. <https://doi.org/10.1016/j.molliq.2015.03.026>.
- [10] Joseph, C. G., Taufiq-Yap, Y. H., Puma, G. L., Sanmugam, K., and Quek, K. S. 2015 "Photocatalytic Degradation of Cationic Dye Simulated Wastewater Using Four Radiation Sources, UVA, UVB, UVC and Solar Lamp of Identical Power Output." *Desalination and Water Treatment* 57: 7976-87. <https://doi.org/10.1080/19443994.2015.1063463>.
- [11] Lu, Z., Wang, Q., Yin, R., and Binmeng, C. 2016. "A Novel TiO₂/Foam Cement Composite with Enhanced Photodegradation of Methyl Blue." *Construction and Building Materials* 129: 159-62. <https://doi.org/10.1016/j.conbuildmat.2016.10.105>.
- [12] Mamulová Kutlákova, K., Tokarsky, J., Kovár, P., Vojtesková, S., Kovárová, A., Smetana, B., Kukutschová, J., Capková, P., and Matejka, V. 2011. "Preparation and Characterization of Photoactive Composite Kaolinite/TiO₂." *Journal of Hazardous Materials* 188: 212-20. <https://doi.org/10.1016/j.jhazmat.2011.01.106>.
- [13] Lakshmi, S., Renganathan, R., and Fujita, S. 1995. "Study on TiO₂-Mediated Photocatalytic Degradation of Methylene Blue." *Journal of Photochemistry and Photobiology A: Chemistry* 88: 163-7. [https://doi.org/10.1016/1010-6030\(94\)04030-6](https://doi.org/10.1016/1010-6030(94)04030-6).
- [14] Falah, M., Mackenzie, K. J. D., Knibbe, R., Samuel, J. P., Hanna, J. V. 2016. "New Composites of Nanoparticle Cu (I) Oxide and Titania in a Novel Inorganic Polymer (Geopolymer) Matrix for Destruction of Dyes and Hazardous Organic Pollutants." *Journal of Hazardous Materials* 318: 772-82. <https://doi.org/10.1016/j.jhazmat.2016.06.016>.
- [15] Li, C. M., He, Y., Tang, Q., Wang, K. T., and Cui, X. M. 2016. "Study of the Preparation of CdS on the Surface of Geopolymer Spheres and Photocatalyst Performance." *Materials Chemistry and Physics* 178: 204-10. <https://doi.org/10.1016/j.matchemphys.2016.05.013>.
- [16] Fallah, M., Mackenzie, K. J. D., Hanna, J. V., and Page, S. J. 2015. "Novel Photoactive Inorganic Polymer Composites of Inorganic Polymers with Copper (I) Oxide Nanoparticles." *Journal of Materials Science* 50: 7374-83. <https://doi.org/10.1007/s10853-015-9295-3>.
- [17] Zhang, Y. J., Liu, L. C., Xu, Y., and Wang, Y. C. 2012. "A New Alkali-Activated Steel Slag-Based Cementitious Material for Photocatalytic Degradation of Organic Pollutant from Waste Water." *Journal of Hazardous Materials* 209-210: 146-50. <https://doi.org/10.1016/j.jhazmat.2012.01.001>.
- [18] Masliana, M., Kenneth, J. D. M., Meor Yusoff, M. S., Wilfred, S. P., and Nur Aqilah, S. 2013. "Degradation of Methylene Blue via Geopolymer Composite Photocatalysis." *Solid State Science and Technology* 21: 23-30. <http://myjms.mohe.gov.my/index.php/masshp/article/view/4602>.
- [19] Zhang, Y., and Liu, L. 2013. "Fly Ash-Based Geopolymer as a Novel Photocatalyst for Degradation of Dye From Wastewater." *Particuology* 11: 353-8. <https://doi.org/10.1016/j.partic.2012.10.007>.
- [20] Khan, M. I., Min, T. K., Azizli, K., Sufian, S., Ullah, H., and Man, Z. 2015. "Effective Removal of Methylene Blue from Water Using Phosphoric Acid Based Geopolymers: Synthesis, Characterizations and Adsorption Studies." *Royal Society of Chemistry Advances* (75): 61410-20. <https://doi.org/10.1039/C5RA08255B>.
- [21] Weinstein, M. P., Turnidge, J. D., Zimmer, B. L., Cockerill, F. R., Wiker, M. A., Traczewski, M. M., Alder, J., Dudley, M. N., Eliopoulos, G. M., Ferraro, M. J., Hardy, D. J., Hecht, D. W., Hindler, J. A., Thomson, R. B., Patel, J. B., and Swenson, J. M. 2018. *Methods for Dilution Antimicrobial Susceptibility Tests for Bacteria that Grow Aerobically*. 11th ed., CLSI standard M07. Wayne, PA: Clinical and Laboratory Standards Institute.
- [22] Francolini, I., Piozzi, A., and Donelli, G. 2014. "Efficacy Evaluation of Antimicrobial Drug-Releasing Polymer Matrices." *Microbial Biofilms Methods in Molecular Biology* 1147: 215-25.
- [23] Beaudoin, J. J., Patarachao, B., Raki, L., and Alizadeh, R. 2011. "Adsorption of Methylene Blue as a Descriptor of C-S-H Nanostructure." *Cement and Concrete Composites* 33: 246-50. <https://doi.org/10.1016/j.cemconcomp.2010.10.011>.
- [24] Otsuki, S., and Adachi, K. 1993. "Metachromasy in Polymer Films. Changes in the Absorption Spectrum of Methylene Blue in Nafion Films by Hydration." *Polymer Journal* 25: 1107-12. <https://doi.org/10.1295/polymj.25.1107>.
- [25] Falah, M., and Mackenzie, K. J. D. 2015. "Synthesis and Properties of Novel Photoactive Composites of P25 Titanium Dioxide and Copper (I) Oxide with Inorganic Polymers." *Ceramics International* 41: 13702-8. <https://doi.org/10.1016/j.ceramint.2015.07.198>.
- [26] Wohlrab, S., Hoppe, R., Schulz-Ekloff, G., and Wöhrle, R.

- D. 1992. "Encapsulation of Methylene Blue into Aluminophosphate Family Molecular Sieves." *Zeolites* 12: 862-5. [https://doi.org/10.1016/0144-2449\(92\)90063-U](https://doi.org/10.1016/0144-2449(92)90063-U).
- [27] Li, L., Wang, S., and Zhu, Z. 2006. "Geopolymeric Adsorbents from Fly Ash for Dye Removal from Aqueous Solution." *Journal of Colloid and Interface Science* 300: 52-9. <https://doi.org/10.1016/j.jcis.2006.03.062>.
- [28] Ismail, B., Hussain, S., and Akram, S. 2013. "Adsorption of Methylene Blue onto Spinel Magnesium Aluminate Nanoparticles: Adsorption Isotherms, Kinetic and Thermodynamic Studies." *Chemical Engineering Journal* 219: 395-402. <https://doi.org/10.1016/j.cej.2013.01.034>.
- [29] Luukkonen, T., Sarkkinen, M., Kempainen, K., Rämö, J., and Lassi, U. 2016. "Metakaolin Geopolymer Characterization and Application for Ammonium Removal from Model Solutions and Landfill Leachate." *Applied Clay Science* 119: 266-76. <https://doi.org/10.1016/j.clay.2015.10.027>.
- [30] Ho, Y. S., and McKay, G. 1999. "Pseudo-Second Order Model for Sorption Processes." *Process Biochemistry* 34: 451-65. [https://doi.org/10.1016/S0032-9592\(98\)00112-5](https://doi.org/10.1016/S0032-9592(98)00112-5).
- [31] Xing, Y., Li, X., Zhang, L., Xu, Q., Che, Z., Li, W., and Li, K. 2012. "Effect of TiO₂ Nanoparticles on the Antibacterial and Physical Properties of Polyethylene-Based Film." *Progress in Organic Coatings* 73: 219-24. <https://doi.org/10.1016/j.porgcoat.2011.11.005>.
- [32] Galkina, O. L., Sycheva, A., Blagodatskiy, A., Kaptay, G., Katanaev, V. L., Seisenbaeva, G. A., Kessler, V. G., and Agafonov, A. V. 2014. "The Sol-Gel Synthesis of Cotton/TiO₂ Composites and Their Antibacterial Properties." *Surface and Coatings Technology* 253: 171-9. <https://doi.org/10.1016/j.surfcoat.2014.05.033>.